ADVANCED MATERIALS
www.advmat.de

Flow Rate Affects Nanoparticle Uptake into Endothelial Cells

*Yih Yang Chen, Abdullah Muhammad Syed, Presley MacMillan, Jonathan V. Rocheleau, and Warren C. W. Chan**

Nanoparticles are commonly administered through systemic injection, which exposes them to the dynamic environment of the bloodstream. Injected nanoparticles travel within the blood and experience a wide range of flow velocities that induce varying shear rates to the blood vessels. Endothelial cells line these vessels, and have been shown to uptake nanoparticles during circulation, but it is difficult to characterize the flow-dependence of this interaction in vivo. Here, a microfluidic system is developed to control the flow rates of nanoparticles as they interact with endothelial cells. Gold nanoparticle uptake into endothelial cells is quantified at varying flow rates, and it is found that increased flow rates lead to decreased nanoparticle uptake. Endothelial cells respond to increased flow shear with decreased ability to uptake the nanoparticles. If cells are sheared the same way, nanoparticle uptake decreases as their flow velocity increases. Modifying nanoparticle surfaces with endothelial-cell-binding ligands partially restores uptake to nonflow levels, suggesting that functionalizing nanoparticles to bind to endothelial cells enables nanoparticles to resist flow effects. In the future, this microfluidic system can be used to test other nanoparticle–endothelial cell interactions under flow. The results of these studies can guide the engineering of nanoparticles for in vivo medical applications.

Nanoparticles are a promising platform for delivering anticancer drugs directly to tumors and sparing the body from off-target organ toxicity.[1,2] Upon systemic administration, nanoparticles will enter the bloodstream, circulate throughout the body and extravasate out of the blood vessel into the tumor to deliver their drug cargo.[3,4] However, many of the in vitro studies performed to characterize therapeutic nanoparticles do not recapitulate the dynamic environment of the bloodstream. Currently, the vast body of work in the literature involve statically incubating nanoparticles with in vitro cultures, which can artificially alter the amount of uptake into cancer cells.[5] Since standard in vitro models lack the fluid flow characteristic of the bloodstream, nanoparticles can settle onto the cells and induce uptake.[5] In vivo, the transport of these nanoparticles would depend on the flow rate of the bloodstream, which may impact their overall biodistribution.[6,7] Additionally, in vitro assays often place nanoparticles in direct contact with cancer cells, ignoring the endothelial cells that nanoparticles would interact with in vivo. The nanoparticle–endothelial cell interaction is important to characterize, since a recent study has found that up to 97% of nanoparticles found in the tumor enter through trans-endothelial processes.[8] Endothelial cells are also mechanically responsive,[9,10] which may influence their propensity to uptake nanoparticles when they experience varying flow shear. The influence of shear is important in the context of tumor vasculature, which is disorganized and leads to varying flow rates.[11–14] The absence of the flow component in traditional assays causes overestimates in the efficacy of nanoparticle therapy in vivo. There are few tools available to study the relationship between flow rate, endothelial cells, and nanoparticle uptake, as shown in

Y. Y. Chen, Dr. A. M. Syed, P. MacMillan, Prof. J. V. Rocheleau, Prof. W. C. W. Chan
Institute of Biomaterials and Biomedical Engineering
University of Toronto
Toronto, Ontario M5S 3G9, Canada
E-mail: warren.chan@utoronto.ca

Y. Y. Chen, Dr. A. Muhammad Syed, P. MacMillan, Prof. W. C. W. Chan
Terrence Donnelly Centre for Cellular and Biomolecular Research
University of Toronto
Toronto, Ontario M5S 3E1, Canada

Prof. J. V. Rocheleau
Department of Physiology
University of Toronto
Toronto, Ontario M5S 1A8, Canada

The ORCID identification number(s) for the author(s) of this article can be found under https://doi.org/10.1002/adma.201906274.

Prof. J. V. Rocheleau
Toronto General Research Institute
University Health Network
Toronto, Ontario M5G 2M9, Canada

Prof. W. C. W. Chan
Department of Chemical Engineering and Applied Chemistry
University of Toronto
Toronto, Ontario M5S 3E5, Canada

Prof. W. C. W. Chan
Department of Material Science and Engineering
University of Toronto
Toronto, Ontario M5S 1A1, Canada

P. MacMillan, Prof. W. C. W. Chan
Department of Chemistry
University of Toronto
Toronto, Ontario M5S 3H6, Canada

DOI: 10.1002/adma.201906274

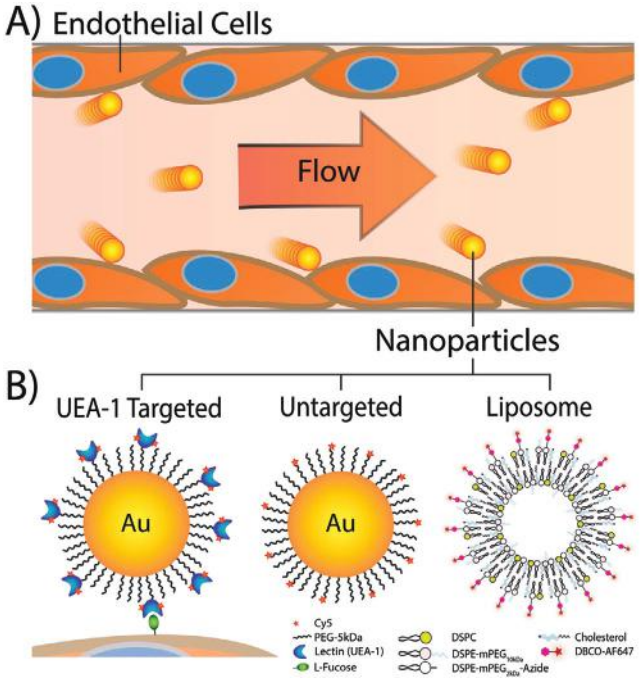

Figure 1. Nanoparticle–endothelial cell interactions under flow. A) Schematic depicting nanoparticles interacting with endothelial cells lining the blood vessel as they flow in the bloodstream. B) Nanoparticle designs used in the study. DSPC: 1,2-distearoyl-sn-glycero-3-phosphocholine; DSPE: 1,2-distearoyl-sn-glycero-3-phosphoethanolamine; DBCO: dibenzocyclooctyne; PEG: polyethylene glycol; UEA-1: Ulex Europaeus Agglutinin-1.

Figure 1. Here, we developed a microfluidic system that allowed us to control the fluid flow of circulating nanoparticles as they interact with endothelial cells. We grew a mature endothelium within the channels of the microfluidic device, and characterized if increasing the flow rate of nanoparticles in solution will decrease their uptake into endothelial cells.

We started developing our microfluidic system (shown in **Figure 2**) by growing an endothelial lining inside the microfluidic device. Using microfluidic technology gives us control over the fluid flow rates and the shear stress that endothelial cells would experience while exposed to nanoparticles. In order for the cells to generate physiologically relevant data, they must mimic certain characteristics of in vivo endothelial cells. In our system, we ensured that our endothelial cells were shear-adapted and formed tight-junctions, similar to physiological blood vessels.[15–18] As shown in **Figure 3**A, we seeded human umbilical vein endothelial cells (HUVECs, Angioproteomie, CAP-0001) from passage 1 to 4 into 0.4 mm × 3.8 mm rectangular microfluidic channels (Ibidi, µ-slide VI 0.4, #80606) at 2 million cells mL^{-1}. After the cells adhere to the microfluidic channel, they were incubated under gentle rocking conditions over the course of 5–7 d (Figure 3A-ii), with one media exchange per day. During this period, the HUVECs expressed Vascular Endothelial cadherin proteins (VE-Cadherin, Figure 3B-i–iii), and grew to ≈95% confluence within 48 h (Figure 3C-i). VE-Cadherin is produced in the perinuclear regions of the cell before being delivered to the cell membranes[19] to crosslink with neighboring cells.[15] Once these proteins crosslink with those of neighboring HUVECs, they form adherens junctions[15,16] and assist in the formation

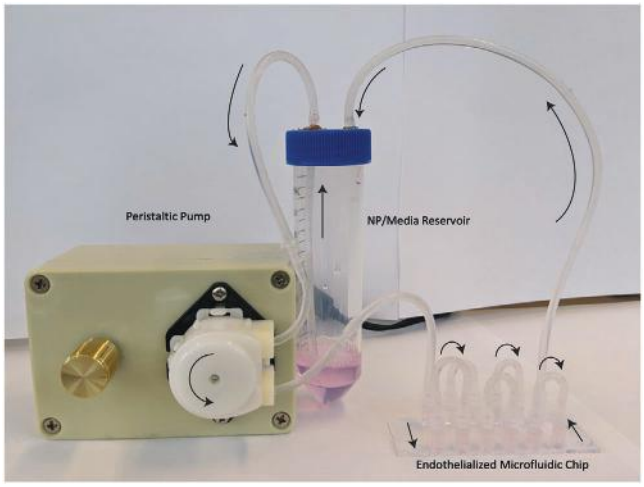

Figure 2. Microfluidic chip connected to a peristaltic pump and media reservoir. Arrows show the direction of fluid flow. The pump withdraws media from the reservoir, pumps it into the microfluidic channels that are connected in series, which then returns the media to the Falcon tube to replenish the reservoir.

of tight junctions. This allows the endothelial cells to remain attached to the chip even when subjected to high shear from fast fluid flow. We quantified the maturity of our endothelial lining by measuring the VE-Cadherin fluorescence signal on the HUVEC membranes and dividing it by the fluorescence found within the perinuclear regions (Figure 3C-ii). A ratio of 1:1 would mean that VE-Cadherin expression is relatively homogenous within the cell, indicating that the HUVECs have not formed tight-junctions. A ratio greater than 1 would indicate that most of the VE-Cadherin signal is along the cell membranes, forming tight junctions. We found that after 5 d of incubation, VE-Cadherin expression begins to plateau at a ratio of ≈3.5:1 in our system. Therefore, we decided to allow the HUVECs to mature for at least 5 d in all subsequent studies in our system so that they remain attached to the chip when we increase the flow rate of the media.

In order to simulate conditions that these cells would experience in the bloodstream, we chose a range of flow rates that would result in shear stresses ranging from 2 to 8 dyn cm^{-2}, which falls within the physiologically relevant range of capillary shear stress.[20] This corresponds to a flow rate from 1.5 to 5.0 mL min^{-1} in our system.[21] It was important for us to match capillary shear stresses because many studies in the literature have shown that endothelial cells are mechanically responsive, and will change protein expression profiles when subjected to changing shear stress.[22–26] These phenotypic changes could also affect their propensity to uptake nanoparticles.[27] When we subjected the endothelial cells to these flow rates, their actin fibers align in the direction of flow, indicating that they are adapting to shear.[13] We visualized this by staining actin using phalloidin-488 (ThermoFisher, #A12379), and quantified fiber alignment through image analysis. Figure 3B-vi shows the actin filaments aligning vertically, in the direction of flow. We applied a range of flow rates from static to 5 mL min^{-1}. We wrote a MATLAB script that identifies actin fibers, determines their orientation, and counts the number of fibers that lay within 45° of normal. Roughly 50% of their actin filaments would lay within 45° if cells are not aligned

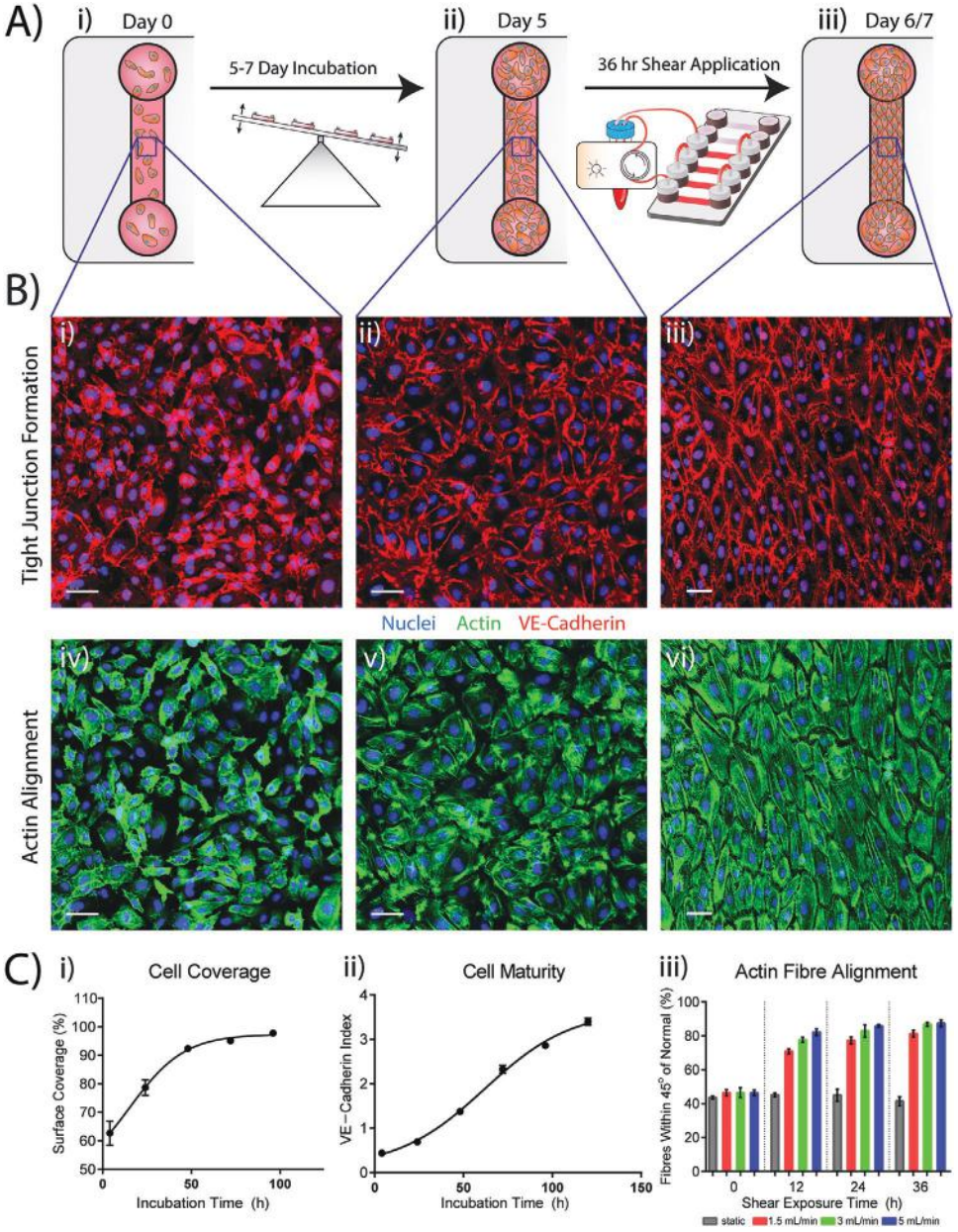

Figure 3. Endothelium device preparation. A-i) Cells are seeded and grown to confluence over 5–7 d and A-ii) are sheared for 36 h at 5 mL min^{-1}, resulting in A-iii) shear-adapted endothelium. B) HUVECs are stained to visualize their nuclei (DAPI, blue), actin filaments to verify shear adaptation (phalloidin-488, green), and VE-Cadherin to verify an intact endothelium (anti-VE-Cadherin-cy3, red). In (B-i), cells begin expressing VE-Cadherin, which migrates to the cell membranes in (B-ii), forming junctions that allow them to resist high shear in (B-iii). In (B-iv,v), actin can be visualized, and fibers will align with the direction of flow in (B-vi). In (C-i), cells grow to above 90% confluence after 48 h of incubation, and the endothelium maturity is quantified in (C-ii) which shows the ratio between membrane-bound VE-Cadherin to perinuclear VE-Cadherin. Actin fiber alignment is quantified in (C-iii), where fibers within 45° of flow direction increase from ≈50% to ≈85% after cells are aligned with fluid flow. Scale bars are 50 µm.

and are relatively circular. Indeed, the fiber alignment is 47% when cells are left at static conditions. After applying shear stress at higher flow rates, fiber alignment increases to > 70% within the first 12 h (Figure 3C-iii). Higher flow rates align the cells faster, with 5 mL min^{-1} reaching ≈80% alignment after only 12 h of shear. Fiber alignment plateaus at ≈85% at 36 h at the highest flow rate of 5 mL min^{-1} in our system. After quantifying the maturity and HUVEC alignment in our system, we were confident that our endothelial cells are metabolically active and shear responsive.

Using this system, we perfused 100 nm gold nanoparticles at different flow rates and quantified the amount of uptake into endothelial cells through confocal microscopy. To synthesize the nanoparticles, we first produced 15 nm gold nanoparticles through the citrate-reduction protocol.[28] These nanoparticles were used as seeds for a second reduction reaction using hydroquinone, until the nanoparticles grew to 100 nm in diameter. The 100 nm gold nanoparticles were surface conjugated with Ulex Europaeus Agglutinin I (UEA-1) lectin, which binds

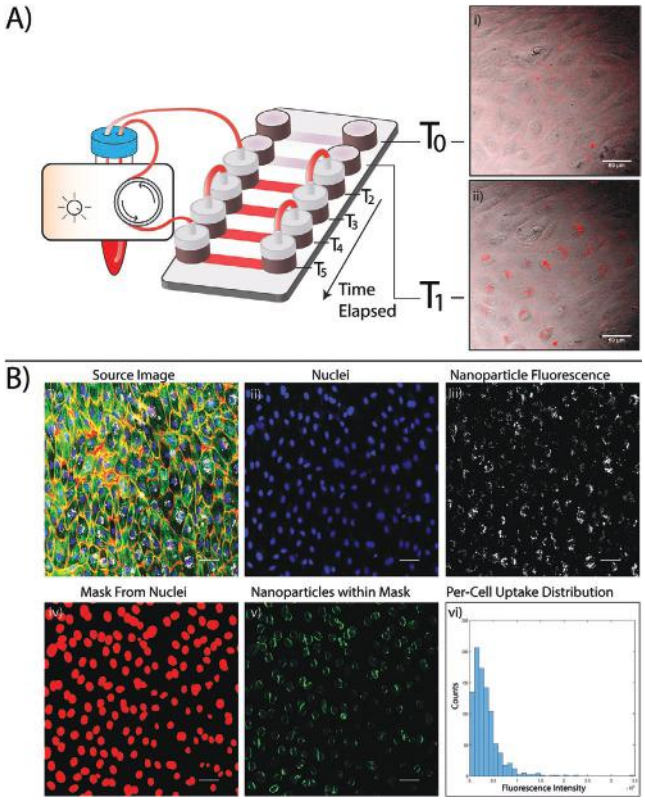

Figure 4. Quantification of nanoparticle fluorescence in HUVECs. A) Nanoparticles are infused into the microfluidic endothelium device, and time points are acquired by disconnecting a channel from the circuit before fixing and staining the cells. A-i,ii) HUVECs gather nanoparticles into the area around their nuclei as time progresses (see Video S1, Supporting Information). Therefore, we stain and image the HUVECs in (B-i). We label the nuclei with DAPI (blue), the actin with phalloidin-488 (green), and the VE-Cadherin with anti-VE-Cadherin-cy3 (red), and nanoparticle fluorescence is shown in white. Using this source image, we extract: B-ii) the DAPI/nuclei channel, and B-iii) the nanoparticle fluorescence channel. B-iv) A mask is produced out of the nuclei channel, and B-v) overlaid over the nanoparticle fluorescence channel. When the fluorescence is plotted on a histogram in (B-vi), their distribution is lognormal. Therefore, we obtain the geometric mean of the fluorescence intensities of each cell as a metric of comparison between different nanoparticle exposure and flow rate conditions. Scale bars are 50 μm.

to human endothelial cells.[29] We back-filled the remaining surface area with 5 kDa polyethylene glycol. UEA-1 lectin was labeled with the dye molecule cy5-NHS to fluorescently tag the gold nanoparticles. The fluorescence enabled us to track and quantify cellular uptake.

After infusing nanoparticles into the endothelium-on-a-chip, we imaged the chip through confocal microscopy and quantified nanoparticle uptake through image analysis. In our studies, and shown in **Figure 4**A, we observed that endothelial cells gather the nanoparticles into their perinuclear regions upon uptake (Video S1, Supporting Information). Therefore, we decided to quantify the amount of nanoparticle uptake in each cell by measuring the Cy5 fluorescence intensity in each perinuclear region. Using the source image obtained through confocal microscopy (Figure 4B-i), we identified the perinuclear regions by staining the HUVEC nuclei with 4′,6-diamidino-2-phenylindole (DAPI, Figure 4B-ii), and wrote a MATLAB script to use the DAPI signal to generate a mask of cell locations (Figure 4B-iv). We extracted the nanoparticle fluorescence channel (Figure 4B-iii), and overlaid this mask atop the nanoparticle fluorescence channel (Figure 4B-v) to quantify the signal intensity within each perinuclear region. This determines the total fluorescence intensity of each cell, which shows a log-normal distribution when plotted on a histogram in Figure 4B-vi. Since this was not a normal distribution, we compared nanoparticle uptake by comparing the geometric means of fluorescence intensity across cell populations, and performed our statistical analysis using Kruskal–Wallis non-parametric tests to determine significance.

Using this procedure, we wanted to determine if shearing the endothelial cells under different flow rates would change their uptake of nanoparticles. HUVECs are known to change protein expression while undergoing shear stress, and it is possible that their propensity to uptake nanoparticles will also change. If we were to infuse nanoparticles at varying flow rates, we would be unable to determine if changes in uptake are due to the effects of nanoparticles' flow speed, or because of phenotypic changes in the endothelial cells. To decouple these two effects, we decided to shear the endothelial cells at different flow rates, then expose them to nanoparticles at static conditions. We subjected 4 endothelial chips to 24 h of 5 mL min^{-1} shear, then changed the flow rates to 0.0 (static), 1.5, or 3 mL min^{-1}, with one device remaining at 5 mL min^{-1}. At every 12 h after the initial 24 h of 5 mL min^{-1} shear, we removed a channel from circulation in each device and injected lectin-targeted 100 nm gold nanoparticles at 0.01×10^{-9} M. We chose to use targeted 100 nm gold nanoparticles because their uptake into endothelial cells is faster, giving us more time resolution in our kinetics curves. The nanoparticles were left in the channel for 4 h in static conditions, after which the cells were rinsed with PBS and fixed with 10% neutral-buffered formalin (Sigma Aldrich, HT501128). Cells were imaged and their nanoparticle uptake was quantified. As shown in **Figure 5**A, when HUVECs experience higher shear stress, they uptake fewer nanoparticles. For example, there is a significant decrease in uptake when HUVECs are exposed to 5 mL min^{-1} of flow, compared to statically cultured HUVECs at the same time point. When HUVECs are sheared for longer, they also decrease their propensity to uptake nanoparticles. This is shown in Figure 5B, where images of HUVECs sheared at 5 mL min^{-1} show a decrease in nanoparticle signal around the perinuclear regions of each cell as shearing time progresses.

These data suggest that heterogeneity in nanoparticle distribution within the tumor vasculature may be due to varying phenotypic profiles of endothelial cells. Some regions of the tumor vasculature may experience more shear stress than others, leading to heterogeneous mechanical responses that lead to varying levels of nanoparticle uptake. In our system, we were able to find a plateau between the 12 and 36 h time points at an applied flow rate of 5 mL min^{-1}. If we perform our nanoparticle uptake experiments within this 24 h time span, any changes in uptake would depend solely on nanoparticle flow speed.

With these shearing conditions in mind, our next step was to determine if the flow velocity of nanoparticles in solution affect their uptake into endothelial cells. We prepared HUVECs in microfluidic devices and applied 5 mL min^{-1} flow

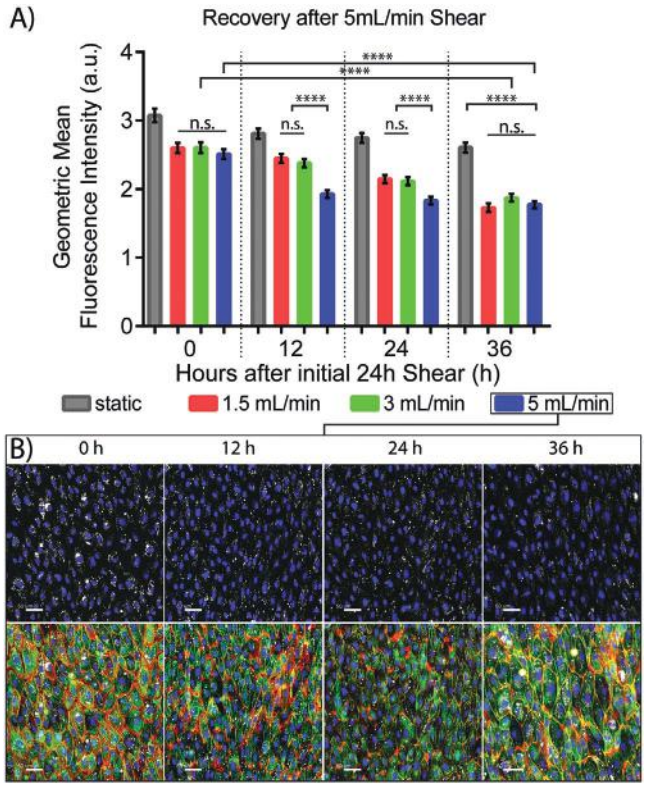

Figure 5. HUVEC uptake of nanoparticles changes upon shear adaptation. A) When HUVECs are subjected to greater shear rates, their ability to uptake nanoparticles decreases. Bars show geometric mean of fluorescence intensity with 95% confidence intervals. Kruskal–Wallis nonparametric tests were used to determine significance. B) Images of HUVECs sheared at 5 mL min^{-1} at time points after the initial 24 h at 5 mL min^{-1}. The amount of nanoparticle uptake stabilizes after a total of 36 h at 5 mL min^{-1}. DAPI stains nuclei (blue); Phalloidin-488 stains actin (green); anti-VE-Cadherin antibody (red); nanoparticle fluorescence signal (white). Scale bars are 50 µm.

rates for 36 h, then exposed them to nanoparticles in media at static, 1.5, 3, and 5 mL min^{-1} flow rates over the course of 15 h. At every 3 h time point, we disconnected a channel in each device from the flow circuit and fixed with 10% neutral-buffered formalin. After the entire time series was concluded, we stained the cells, imaged them, and quantified their nanoparticle uptake. When UEA-1 targeted nanoparticles are incubated in static conditions with HUVECs, they show appreciable uptake at 12 h (**Figure 6**A,B). However, when flow is introduced, this uptake is significantly reduced (Figure 6C,D). When we quantified the uptake across all flow rates and time points, we found a general trend where increases in nanoparticle flow rate leads to decreases in endothelial cell uptake, as shown in Figure 6E. This suggests that for uptake to occur, nanoparticles need to have a certain residence time on the cell membrane surface. If the flow rate was increased, individual nanoparticles would experience a decrease in residence time, and thereby decreasing nanoparticle uptake.

The residence time parameter would also be affected by the nanoparticle binding affinity to the cell membrane.[30] A stronger binding affinity would allow the nanoparticle to resist the flow forces of the solution, which would increase the amount of interaction time with the cell membrane. To see if the residence time depends on the nanoparticle affinity to the cell surface, we further compared the effect of flow on nanoparticle uptake for targeted and nontargeted nanoparticles. If we were to remove the affinity or "stickiness" of the nanoparticles to the cell surface, we hypothesized that the effect of flow on nanoparticle uptake would be much greater, leading to a sharper decrease in uptake as flow velocity is increased. When we compared HUVECs that were incubated with untargeted nanoparticles statically, we still found uptake at 12 h (Figure 6F,G). However, when flow was introduced, nanoparticle uptake was not detectable (Figure 6H,I). Comparing all flow rates and time points in Figure 6J shows that when 100 nm gold nanoparticles are no longer targeted to endothelial cells, the effect of flow rate on nanoparticle uptake is so drastic that only statically incubated nanoparticles show appreciable amounts of uptake into endothelial cells. The introduction of a low 1.5 mL min^{-1} flow rate decreases the uptake of the nanoparticles by ≈20-fold at 17 h, in geometric mean intensity of fluorescence (Figure 6J). The data presented here aligns with previous work by Cho et. al, which shows that the settling of nanoparticles on the cell membrane encourages uptake.[5] Here, when flow is introduced to "wash away" the nanoparticles, uptake is drastically reduced unless the nanoparticles are modified to "stick" to the surface.

We were curious if faster flow rates also affected the uptake of organic nanoparticles into endothelial cells. Since one of the most clinically successful nanoparticles is the liposome, we used our device to test if faster flow rates also decreased liposome uptake into endothelial cells. We synthesized 126 nm liposomes and labeled them with Alexa Fluor 647, repeated the experiment in Figure 5 by shearing our endothelial cells at 5 mL min^{-1}. At 12 h time points, we disconnected a channel from the flow circuit and exposed the cells in that channel to 8×10^{-9} M of liposomes in static conditions for 4 h. As shown in Figure S2 (Supporting Information), liposome uptake decreased after 12 h of shear and remained constant for the next 24 h. Therefore, increased flow rates also condition the endothelial cells to decrease their liposome uptake.

Interestingly, when we sheared the endothelial cells for 12 h, and then started our liposome uptake experiments under different flow rates, we found that the uptake of liposomes was not affected by flow conditions, except at 6–9 h where increases to flow rate increase liposome uptake. This difference disappears after 12 h, as seen in Figure S3 (Supporting Information). It is possible that denser, inorganic nanoparticles are more affected by flow than lighter, organic nanoparticles. However, increased flow rate still induces a lower nanoparticle uptake in endothelial cells by changing their phenotype.

There remains a lack of understanding regarding the behavior of nanoparticles once they are administered into the body. Flow is a fundamental property of blood that can dictate the delivery and exposure of nanoparticles to different cells in the body. However, flow is rarely a condition that is examined as it is difficult to study in animals. Our platform was able to show the impact of flow on the interactions between cells and nanoparticles. We found that there is an inverse relationship between flow rate and cell uptake within the flow rates studied. We also found that using targeting agents to bind to endothelial cells can mitigate some of the impact of flow rate. To generalize these statements, there is a need to

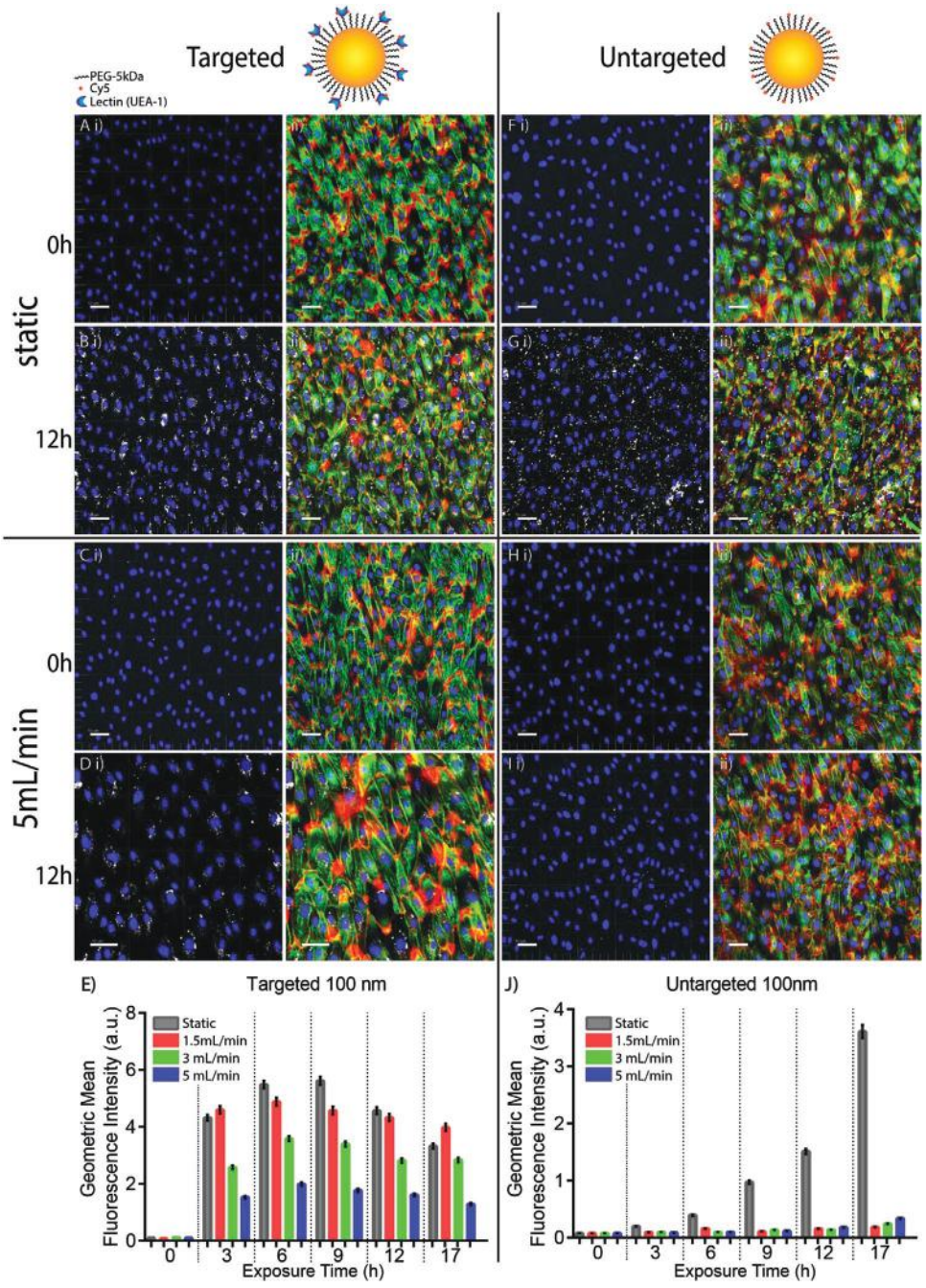

Figure 6. Increasing nanoparticle flow rate decreases uptake. (A)–(H) depict the nuclei (DAPI, blue) and nanoparticle (Cy5, white) channels, F-actin (phalloidin-488, green), and VE-Cadherin (Cy3, red). (A) and (B) show the targeted nanoparticle uptake at static conditions at time 0 and 12 h, respectively. (C) and (D) show targeted nanoparticle uptake at 5 mL min^{-1} flow rate at 0 and 12 h. (E) shows the geometric mean of fluorescence intensity across all flow rates and all time points. For untargeted nanoparticle uptake, (F) and (G) show uptake at static conditions at 0 and 12 h, and (H) and (I) show uptake when 5 mL min^{-1} flow rate is applied for 0 and 12 h. (J) shows geometric mean intensity of all time points and all flow rates for untargeted nanoparticles. Error bars are 95% confidence intervals. Kruskal–Wallis nonparametric tests were used to determine significance. Without targeting the nanoparticles to the endothelial cells, any amount of flow rate will drastically inhibit nanoparticle uptake. Scale bars are 50 µm.

evaluate the impact of flow on large libraries of nanoparticles of different size, shape, and chemical composition. This is important because the ability to control the cellular accumulation of nanomaterials is important for noninvasive imaging for early detection or for treatment of disease. This is a first-generation microfluidic system designed to explore the effects of flow rate on nanoparticle–cell interactions. Although it is a simple design that allows researchers to evaluate this relationship, blood vessels are more complex in vivo. For example, tumor vasculatures exhibit chaotic tortuosity, which

heterogeneously changes the blood flow rate throughout the tumor. Future microfluidic systems would need to include more complex microfluidic structures to mimic this tortuous vasculature. Such devices are needed to perform fundamental studies on the interactions of nanoparticles with biological systems. This information is critical for designing nanomaterials for medical applications.

Supporting Information

Supporting Information is available from the Wiley Online Library or from the author.

Acknowledgements

Y.Y.C. and A.M.S. would like to thank the Natural Sciences and Engineering Research Council of Canada (NSERC). Y.Y.C. also thanks Kristi Piia Callum Memorial Fellowship, and Teresina Florio Memorial Fellowship for funding support. P.M. would like to thank the Walter C. Sumner Memorial Fellowship for the funding. W.C.W.C. acknowledges NSERC Grant 2015–06397, Collaborative Health Research Program Grant CPG-146468, Canadian Institute of Health Research Grants FDN-159932 and MOP-1301431, Canadian Research Chairs Program Grant 950–223824, and Canadian Cancer Society Grant 705285-1. All data and materials are available within the manuscript or Supporting Information.

Conflict of Interest

The authors declare no conflict of interest.

Author Contributions

Y.Y.C. and W.C.W.C. designed research; Y.Y.C. performed research, contributed new reagents/analytic tools, and analyzed data; P.M. synthesized and characterized liposomes; Y.Y.C. and A.M.S. wrote the image analysis MATLAB code; and Y.Y.C. and W.C.W.C. wrote the paper. J.V.R. edited the paper.

Keywords

blood vessels, flow shear, flow velocity, microfluidics, nanomedicine, nanoparticles

Received: September 24, 2019
Revised: April 4, 2020
Published online: May 8, 2020

[1] Y.-H. Cheng, C. He, J. E. Riviere, N. A. Monteiro-Riviere, Z. Lin, *ACS Nano* **2020**, *14*, 3075.
[2] L. Brannon-Peppas, J. O. Blanchette, *Adv. Drug Delivery Rev.* **2012**, *64*, 206.
[3] A. Z. Wang, R. Langer, O. C. Farokhzad, *Annu. Rev. Med.* **2012**, *63*, 185.
[4] S. Wilhelm, A. J. Tavares, Q. Dai, S. Ohta, J. Audet, H. F. Dvorak, W. C. W. Chan, *Nat. Rev. Mater.* **2016**, *1*, 16014.
[5] E. C. Cho, Q. Zhang, Y. Xia, *Nat. Nanotechnol.* **2011**, *6*, 385.
[6] A. T. Florence, *J. Controlled Release* **2012**, *164*, 115.
[7] K. M. Tsoi, S. A. Macparland, X. Z. Ma, V. N. Spetzler, J. Echeverri, B. Ouyang, S. M. Fadel, E. A. Sykes, N. Goldaracena, J. M. Kaths, J. B. Conneely, B. A. Alman, M. Selzner, M. A. Ostrowski, O. A. Adeyi, A. Zilman, I. D. McGilvray, W. C. W. Chan, *Nat. Mater.* **2016**, *15*, 1212.
[8] S. Sindhwani, A. M. Syed, J. Ngai, B. R. Kingston, L. Maiorino, J. Rothschild, P. MacMillan, Y. Zhang, N. U. Rajesh, T. Hoang, J. L. Y. Wu, S. Wilhelm, A. Zilman, S. Gadde, A. Sulaiman, B. Ouyang, Z. Lin, L. Wang, M. Egeblad, W. C. W. Chan, *Nat. Mater.* **2020**, *19*, 566.
[9] O. F. Khan, M. V. Sefton, *Biomed. Microdevices* **2011**, *13*, 69.
[10] J. Han, B. J. Zern, V. V. Shuvaev, P. F. Davies, S. Muro, V. Muzykantov, *ACS Nano* **2012**, *6*, 8824.
[11] J. A. Nagy, S. H. Chang, A. M. Dvorak, H. F. Dvorak, *Br. J. Cancer* **2009**, *100*, 865.
[12] J. A. Nagy, H. F. Dvorak, *Clin. Exp. Metastasis* **2012**, *29*, 657.
[13] J. Tan, S. Shah, A. Thomas, H. D. Ou-Yang, Y. Liu, *Microfluid. Nanofluid.* **2013**, *14*, 77.
[14] S. Sindhwani, A. M. Syed, S. Wilhelm, D. R. Glancy, Y. Y. Chen, M. Dobosz, W. C. W. Chan, *ACS Nano* **2016**, *10*, 5468.
[15] M. Giannotta, M. Trani, E. Dejana, *Dev. Cell* **2013**, *26*, 441.
[16] E. S. Harris, W. J. Nelson, *Curr. Opin. Cell Biol.* **2010**, *22*, 651.
[17] E. Dejana, D. Vestweber, *Prog. Mol. Biol. Transl. Sci.* **2013**, *116*, 119.
[18] E. Dejana, E. Tournier-Lasserve, B. M. Weinstein, *Dev. Cell* **2009**, *16*, 209.
[19] S. Almagro, C. Durmort, A. Chervin-Petinot, S. Heyraud, M. Dubois, O. Lambert, C. Maillefaud, E. Hewat, J. P. Schaal, P. Huber, D. Gulino-Debrac, *Mol. Cell. Biol.* **2010**, *30*, 1703.
[20] F. Gentile, M. Ferrari, P. Decuzzi, *Ann. Biomed. Eng.* **2008**, *36*, 254.
[21] Ibidi GmbH, *Shear Stress and Shear Rates for Ibidi Microslides- Based on Numerical Calculations* **2016**.
[22] M. Uematsu, Y. Ohara, J. P. Navas, K. Nishida, T. J. Murphy, R. W. Alexander, R. M. Nerem, D. G. Harrison, *Am. J. Physiol.: Cell Physiol.* **1995**, *269*, C1371.
[23] A. B. Fisher, S. Chien, A. I. Barakat, R. M. Nerem, *Am. J. Physiol.: Lung Cell. Mol. Physiol.* **2001**, *281*, L529.
[24] E. Tzima, M. Irani-Tehrani, W. B. Kiosses, E. Dejana, D. A. Schultz, B. Engelhardt, G. Cao, H. DeLisser, M. A. Schwartz, *Nature* **2005**, *437*, 426.
[25] G. G. Galbraith, R. Skalak, S. Chien, *Cell Motil. Cytoskeleton* **1998**, *40*, 317.
[26] T. Nagel, N. Resnick, W. J. Atkinson, C. F. Dewey, M. A. Gimbrone, *J. Clin. Invest.* **1994**, *94*, 885.
[27] J. N. Topper, M. A. Gimbrone, *Mol. Med. Today* **1999**, *5*, 40.
[28] S. D. Perrault, W. C. W. Chan, *J. Am. Chem. Soc.* **2009**, *131*, 17042.
[29] V. Conrad-Lapostolle, L. Bordenave, C. Baquey, *Cell Biol. Toxicol.* **1996**, *12*, 189.
[30] W. Jiang, B. Y. S. Kim, J. T. Rutka, W. C. W. Chan, *Nat. Nanotechnol.* **2008**, *3*, 145.

